

Acoustically pumped stimulated emission in GaAs/AlGaAs quantum wells

A. B. Nadtochii and O. A. Korotchenkov

Department of Physics, Kiev National University, Kiev 03680, Ukraine

H. G. Grimmeiss

Solid State Physics, University of Lund, Box 118, S-22100 Lund, Sweden

(Received 27 May 2002; revised manuscript received 29 August 2002; published 4 March 2003)

We report on an extremely narrow linewidth of a two-dimensional electron-gas photoluminescence in GaAs/AlGaAs quantum wells pumped by ultrasonic vibrations. Below the threshold pumping amplitude, the observed emission line is weak, broad, and undergoes a redshift consistent with the evolution of an electron-hole plasma recombination in the oscillating piezoelectric fields accompanying the sample vibrations. Above the threshold, a narrow emission line arises, which sharpens up to ~ 0.1 -meV full width at half maximum, and gains intensity with increasing pumping amplitude. Weighing different alternatives, it is suggested that the data are best explained within the framework of stimulated emission originating from the acoustically pumped injection of enhanced electron and hole densities.

DOI: 10.1103/PhysRevB.67.125301

PACS number(s): 78.67.De, 78.45.+h, 78.20.Hp

Acoustic waves have been widely employed to modulate the optical properties of piezoelectric bulk solids such as LiNbO₃ and GaAs,^{1,2} and the impact of acousto-optical techniques seems to be quite far reaching. These techniques applied to semiconductor heterostructures including quantum well (QW) structures appeared very recently to be a subject of increased interest.³⁻⁶ The priory concern behind these efforts is the expectation of the use of acoustic driving techniques for tailoring optoelectronic devices. For example, acoustically tunable lateral potential modulation can be achieved in the plane of a QW by employing piezoelectric fields of acoustic waves, which store the photoexcited carriers into the moving potential and thus can be used for optical signal processing.^{3,6}

It is known that electrons and holes confined to lower-dimensional quantum structures offer superior optical performance.⁷ Carrier confinement to lower dimensions is particularly interesting for low-threshold laser applications. The storage of electron or hole plasma in the piezoelectric potential of acoustic waves is expected to strongly enhance carrier interaction effects in photoluminescence (PL), which may have interesting practical consequences inherent to the occurrence of spontaneous and stimulated emission in semiconductor heterostructures. However, only a few studies have hitherto been performed in this research field. Theoretically, evidence of acoustic pumping effects has been obtained by analyzing a localized quantum dot pumped by stored electrons and holes.⁸ When acoustic waves cross the dot, the stored carriers drop into the dot and form an excitonic state which yields a train of equally spaced photons or lasing. Experimentally, dynamic band-structure modulation and carrier distribution have been shown to profoundly impact PL in QW's.^{4,9}

In this paper, we demonstrate that an extremely narrow PL line can be observed in GaAs/AlGaAs QW structures pumped by ultrasonic vibrations. The occurrence of this line is attributed to the injection of high electron and hole densities due to driving piezoelectric fields between the antinodes of the standing acoustic wave resulting in a stimulated opti-

cal emission. The interest in this kind of research is both fundamental, leading to a better understanding of acoustically affected luminescence in quantum wells, and applied, since one should expect that acoustic driving techniques may be integrated into quantum well microcavity optics yielding different types of light-emitting devices.

The samples used in our experiments were grown by molecular-beam epitaxy. They consist of an n^+ -type (001) GaAs substrate, a 3000-Å GaAs Si-doped (10^{18} cm⁻³) buffer layer, 30 periods of undoped 100-Å GaAs quantum wells separated by 100-Å Al_{0.5}Ga_{0.5}As barriers, and a 300-Å GaAs Be-doped (2×10^{18} cm⁻³) cap layer. The backside Ohmic contacts were formed by alloying AuGe on the substrate.

An Au Schottky contact was evaporated on the top of one of the samples. By biasing the barrier, this sample was used to study the origin of the observed photoluminescence band and to estimate the density n_{2D} of a two-dimensional (2D) electron gas (2DEG) from the evolution of the PL band.¹⁰

Another sample, without Schottky barrier and exhibiting $n_{2D} \approx 2.5 \times 10^{11}$ cm⁻², was used to study the acoustic pumping effect.¹¹ The size of this rectangular sample was about $5 \times 4 \times 0.62$ mm³. Ultrasonic vibrations were achieved by mounting the sample onto the 41° Y-X cut LiNbO₃ piezoelectric plate, as shown in Fig. 1. An AVTECH AV-1015-B pulse generator was employed to feed the plate. Minimizing the temperature rise of the sample, the driving plate was deliberately energized by short pulses of about 1 μs. All spectral measurements were taken with a varying pulse repetition rate and a fixed duty cycle of 20%. By adjusting the length of the plate to that of the sample, a resonant vibrating system exhibiting a set of acoustic modes was achieved. The measurements were then performed at the lowest longitudinal eigenmodes of the sample vibrations, and the maximum vertical displacement of the sample surface was estimated to be of the order of 0.2 nm in the employed frequency range from 300 to 400 kHz. The sample was mounted on a cold finger of a closed cycle refrigerator operated down to 12 K, and the luminescence was detected at or near 30 K. It was excited by

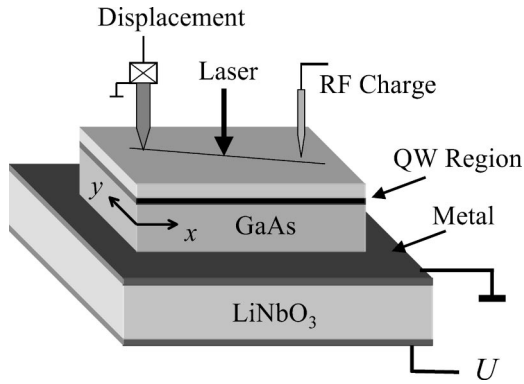


FIG. 1. Sample and measurement schematics. On the left side, the tip for detecting surface displacements is seen. On the right side, the capacitance coupling between the metal tip and the sample used to image the charge flow in the confinement region is shown.

a He-Ne laser and collected in a near-backscattering geometry perpendicular to the QW plane. The exciting light was focused on a region of the order of $200\ \mu\text{m}$ in diameter. The sample could be shifted laterally relative to the optical axis of the double monochromator (SPEX-1680, 1200-g/mm grating) used to disperse the PL. The luminescence signal was detected by employing a Hamamatsu R928 photomultiplier tube followed by either a model 162 boxcar averager or a 72080 Perkin Elmer lock-in amplifier. In the former case, the PL signal was averaged over the aperture that matched the duration of the pump pulse. In the latter case, the PL signal was collected at the repetition frequency of these pulses.

Considering that the redistribution of mobile charges underneath the sample surface is supposed to play a key role in the present study, we compared our luminescence data with maps of surface displacements induced by acoustic vibrations and with the motions of charges underneath. The vertical displacements were taken with a grounded metal tip connected to a calibrated miniature wide-band piezoelectric detector (Fig. 1). The tip was attached to the vibrating surface, and the output rf signal was found to be proportional to the local surface displacement. To monitor the motions of charges induced by the oscillating sample, a sharp metal tip was brought close ($\approx 100\ \mu\text{m}$) to its surface (rf charge in Fig. 1). The flow of charge gave rise to a voltage on the tip on the one side due to the capacitance between the tip and the sample as a whole and on the other side between the tip and the confinement region, which is oscillatory in time with the same frequency as the driving rf signal. The tip rf voltage was then measured by a sensitive amplifier.

While scanning the tip across the surface, the amplitude of the oscillatory signal was mapped, which directly reflected the contours of acoustically distributed charges. In order to correlate the local variations of charge on a subsurface with the luminescence data taken from the QW, we employed a He-Ne laser. By this we provided enhanced charge densities in the confinement region outside the electron-hole generation area, which is due to the drift diffusion of electrons and holes in the plane of the QW. By extracting two images taken with and without laser light, we were able to display contours of charges inherent to the confinement region. With this

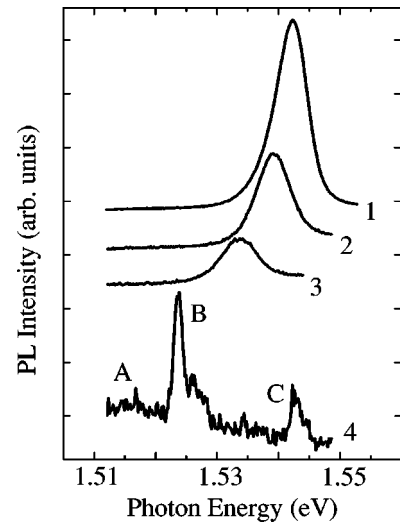


FIG. 2. PL spectra of the GaAs QW taken by a boxcar averager at different pumping amplitudes U : 1–0, 2–30, 3–40, and 4–45 V. The zeros are displaced from top to bottom. Spectrum 4 is enlarged by a factor of 50 for clarity. Full widths at half maximum are 6.4 (spectrum 1), 7.1 (2), 7.9 (3), 1.8 (4, line B), and 2.2 (4, line C) meV.

technique, we avoided artifacts in the images, which could occur because of antenna pickup and ground loop effects. These studies were performed at room temperature, and the spatial resolution in these experiments was $\leq 100\ \mu\text{m}$.

A set of PL spectra is shown in Fig. 2 illustrating the changes in the emission with voltage U applied to the LiNbO₃ transducer. It is seen that acoustic pumping makes the emission line (spectrum 1) progressively weaker in intensity. The line gets broader and undergoes a low-energy shift (spectra 2 and 3), which is reminiscent of the changes in the 2DEG luminescence observed with increasing electron-gas densities.¹⁰ We therefore believe that the observed PL band is due to recombination of an electron plasma and a photoexcited valence-band hole. The changes seen in spectra 2 and 3, compared with spectrum 1, may originate partly from the increased electron density in acoustic fields because of the piezoelectric coupling to the 2DEG,¹² and partly from the sample heating that accompanies the vibrations in GaAs.

Since our main intention has been to study nonthermal phenomena, special care was taken to avoid inaccurate temperature measurements and to make sure that the pumping is not a purely thermal process. As will be seen below, any contribution from a possible heating of the sample can easily be ruled out by carefully analyzing the spectral changes at higher pumping.

Increasing the pumping amplitude U above about 40 V changes the observed emission spectrum quite considerably. The broad PL band of the electron-hole plasma is further quenched and becomes remarkably broader (“A” in spectrum 4 of Fig. 2). Simultaneously, a narrow emission line B appears in the spectral range of the electron-hole plasma recombination together with a line C recovered in the range of the nonpumped PL line shown in spectrum 1. As the pumping amplitude increases further, the peak energy of line B decreases only slightly and its intensity increases (see Fig. 3)

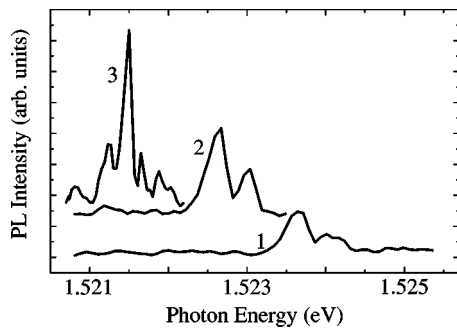


FIG. 3. Evolution of line B in spectrum 4 of Fig. 2 for pumping amplitudes $U=46$ (1), 48 (2), and 50 (3) V. The full width at half maximum is 0.13 meV for the strongest line in spectrum 3. The spectra were taken by a lock-in amplifier. The zeros are displaced from bottom to top.

at the expense of line C until nearly all the intensity is concentrated in one single line. These results cannot be explained by the temperature dependence of the PL band proving that the observed narrow emission is not due to thermal processes.

However, there are good reasons to believe that such a behavior is qualitatively consistent with the redistribution of free carriers in the oscillating piezoelectric potential of the QW plane. Indeed, the unbound electrons in the 2DEG tend to relax in the piezoelectric potential. Since the employed acoustic frequency is much lower than the conductivity relaxation frequency, the bunching of charge in the 2DEG (and variations of n_{2D} in the QW plane), which increases with increasing U , is expected to follow the piezoelectric field distribution and, hence, to form regions of accumulated and depleted electron densities. The height of the entrance slit of the monochromator allows to study the total length of the light-emitting zone of the sample, which is rather large, and to observe simultaneously the PL originating from the region of varying electron-gas density. This should explain the occurrence of a remarkably broadened emission band A with a hardly discernible peak energy in spectrum 4 of Fig. 2 and the observation of line C, which is probably due to a band-to-band electron-hole recombination arising in a low electron-density region. Line C is then expected to be narrower than the emission line in spectrum 1, which is indeed observed, and shifted to higher energies, which is not observed. The unnoticed shift to higher energies may be explained by possible sample heating due to the pumping, which would shift a band-to-band electron-hole recombination to lower energies. As discussed below, the pumping-induced spreading of charge across the QW is a complicated process. With the technique employed, we are unable to correctly map the spatial variations of the emission lines A–C in the plane of the QW. However, the energy position and the emission intensity of the lines are found to change when moving the laser spot across the sample, in qualitative agreement with the model of bunched charges.

The assignment of line B in Fig. 2 is not straightforward. Based on the low-energy shift of this line compared to the band-to-band electron-hole recombination in line C, an exciton origin of line B may be one explanation. However, con-

sidering the heating effect of the pumping on electrons in the 2DEG, the dominance of excitons over the electron-hole plasma seems unlikely. Consistent with this notion is the fact that line B didn't merge with line C when the temperature was slightly increased. This last result taken together with the low emission intensity in line B may be indicative of the involvement of above-barrier heated electrons in the emission of line B. This would imply that the acoustic pumping injects carriers from the low-band-gap GaAs layers into the high-band-gap AlGaAs layers, which then recombine indirectly both in real and momentum space with holes in GaAs QW's. However, the observed evolution of the spectral shape of line B with increasing U weakens the evidence of this assignment. The recombination from higher-energy states of hot electrons would yield a distinct high-energy tail of line B, which is expected to increase with increasing U . However, this is not in agreement with the data shown in Figs. 2 and 3.

We therefore believe that the origin of line B is probably better understood in the framework of stimulated emission occurring in a Coulomb-correlated electron-hole plasma.¹³ In recent studies, Akiyama and co-workers^{13,14} identified the gain mechanism in photoexcited quantum wires, which they showed to be due to recombination in the dense electron-hole plasma peaked in the energy range of the spontaneous recombination of free electrons and holes. Within such an approach, the domains of free electrons and holes in the oscillating driving potential move back and forth in opposite directions inside the plane of the QW's.¹⁵ When the moving electron and hole clouds are allowed to spatially overlap, they form an active region and radiate in a broad emission band. As soon as the injected spatially varying electron and hole densities become high enough for the stimulated emission to occur in the region of overlap, line B arises within the range of the spontaneous emission represented by band A (Fig. 2). Line B gets sharper and sharper from spectrum 1 to spectrum 3 in Fig. 3 accompanied by the development of optical modulation structures, which are best resolved in spectrum 3. They are separated by approximately 0.1 nm and are most likely characteristic of the cavity modes. All these findings are strong indications for the occurrence of stimulated emission.

The validity of the presented model is further supported by the data shown in Fig. 4. The surface vibrations imaged in Fig. 4(a) reveals the regions of high and low vibration amplitudes (white and black areas, respectively). In the acoustically induced charge motion image shown in Fig. 4(b), regions of high and low signals are presented as white and black areas, respectively. The most striking observation is the maximum flow of charges [white areas in Fig. 4(b)] between the antinodes of the standing wave [white regions in Fig. 4(a)]. Consistent with our model we explain the observed contours as follows. Free electrons are collected at the piezoelectric potential maxima (hatched cloud in the inset of Fig. 5). In a half period of the standing wave, the potential phase is reversed (dotted lines), and the electrons are expelled outwards (arrows in the inset). The applied rf pump causes, therefore, the electrons to move back and forth between the

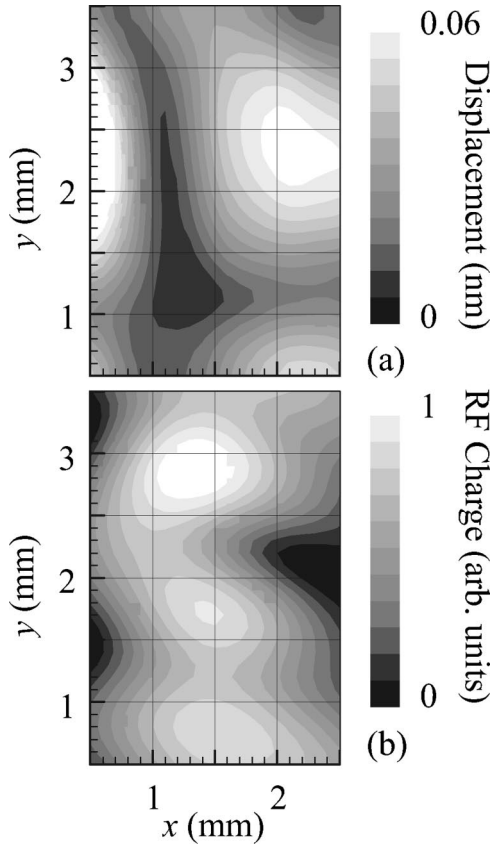


FIG. 4. (a) Vertical displacement image taken from the sample surface. (b) Acoustically driven rf charge image taken in the same region as in (a). The striking laser light is focused at about $x=3$, $y=2$ mm outside the imaged region.

antinodes displayed in Fig. 4(a) as white areas, in very good agreement with the data of Fig. 4(b).

In a more quantitative manner, these results can also be discussed in terms of the electron current density, which is assumed to have the same harmonic time dependence as the driving rf field, $\mathbf{J}(x,y,t) = \mathbf{j}(x,y)\exp(-i\omega t)$, where ω is the vibration angular frequency, and is given by $\mathbf{j} = -\rho_0\mu\nabla\varphi - D\nabla\rho$. Here, μ and D are the electron mobility and diffusivity, respectively, $\varphi(x,y)$ is the piezoelectric potential, and $\rho(x,y)$ is the perturbation in the charge density relative to the equilibrium value ρ_0 . Applying the equation for charge conservation $\partial\rho/\partial t + \nabla\cdot\mathbf{J} = 0$ yields the relation $\mathbf{j}(x,y) = A\nabla\varphi(x,y)$, where A is a constant parameter. We have calculated this relation numerically by starting from Fig. 5(a), which shows the representative displacement field $u(x,y)$ taken around an antinode of the standing wave. By making one further approximation, $\varphi(x,y) = (e/\epsilon)u(x,y)$ with e the piezoelectric constant and ϵ the dielectric constant, we arrive at the current-density distribution shown in Fig. 5(b). Com-

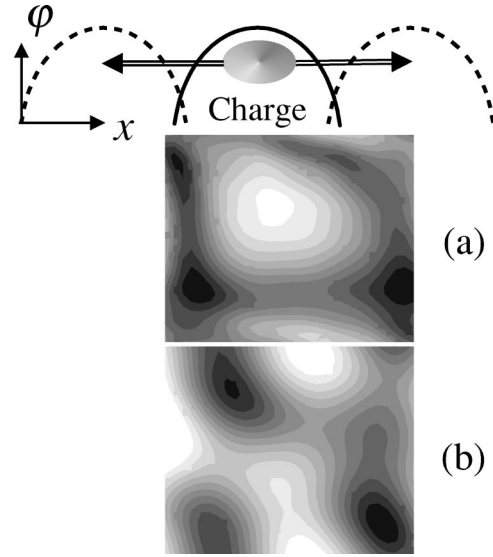


FIG. 5. (a) Representative antinode of the surface displacement. Black to white corresponds to increasing displacement amplitudes. (b) Numerically computed electron current density (see text for details). Inset: schematics of the piezoelectric potential distribution across the x axis at times $t=0$ (solid line) and $t=T/2$ (dotted lines) with T as the standing-wave period.

paring Figs. 4(b) and 5(b), it is readily seen that the maps are in reasonable agreement thus proving that the charge flow indeed moves away from the displacement antinodes. In a similar manner, our PL exhibited a distinct enhancement of the sharp-line emissions (cf. Fig. 3) between the antinodes of the standing wave, in good agreement with our model. Indeed, the overlap of electron and hole wave functions is expected to increase rather distinctly just between the antinodes because this is clearly the region where the electron and hole clouds, moving in the opposite directions, would overlap.

To conclude, we have observed a remarkable narrowing of the 2DEG luminescence line in acoustically pumped GaAs/AlGaAs quantum well structures. Weighing different alternatives, it is suggested that one of the most probable explanations for the narrowing of the line is the occurrence of stimulated emission. We believe that the presented data upgrade the importance of acoustic pumps for exploring lasing in semiconductors well beyond mere promises. Further investigations are needed to optimize the cavity design and to demonstrate acoustically driven lasing.

One of us (O.A.K.) would like to thank the Department of Physics, Seoul National University, for support through the BK21 Program during which a course of spectral measurements was performed. The authors like to thank the Swedish Foundation for the Promotion of Semiconductor Physics for financial support.

¹C. S. Tai, *Guided-Wave Acousto-Optics: Introduction, Devices and Applications* (Springer, New York, 1990).

²A. Korpel, *Acousto-Optics* (Marcel Dekker, New York, 1997).

³C. Roake, S. Zimmermann, A. Wixforth, J. P. Kotthaus, G. Böhm,

and G. Weimann, *Phys. Rev. Lett.* **78**, 4099 (1997).

⁴T. Sogawa, P. V. Santos, S. K. Zhang, S. Eshlaghi, A. D. Wieck, and K. H. Ploog, *Phys. Rev. B* **63**, R121307 (2001).

⁵O. A. Korotchenkov, A. Yamamoto, T. Goto, M.-W. Cho, and T.

- Yao, Appl. Phys. Lett. **74**, 3179 (1999).
- ⁶M. Streibl, A. Wixforth, and A. C. Gossard, Appl. Phys. Lett. **75**, 4139 (1999).
- ⁷C. Weisbuch and B. Vinter, *Quantum Semiconductor Structures* (Academic, San Diego, 1991).
- ⁸C. Wiele, F. Haake, C. Rocke, and A. Wixforth, Phys. Rev. A **58**, R2680 (1998).
- ⁹F. Alsina, P. V. Santos, R. Hey, A. García-Cristóbal, and A. Cantarero, Phys. Rev. B **64**, R041304 (2001).
- ¹⁰See, e.g., A. J. Shields, M. Pepper, D. A. Ritchie, and M. Y. Simmons, Adv. Phys. **44**, 47 (1995).
- ¹¹We recognize that this value is an average over all QW's. We believe that the density variation in different QW's broadens the observed PL lines. Although details of the variation have not been studied in this work, the consistency of the results has been checked by using another sample with 20 QW's. The pumping effect on the PL band was found to be qualitatively similar.
- ¹²See, e.g., A. Wixforth, J. Scriba, M. Wassermeier, J. P. Kotthaus, G. Weimann, and W. Schlapp, Phys. Rev. B **40**, 7874 (1989).
- ¹³H. Akiyama, L. N. Pfeiffer, M. Yoshita, A. Pinczuk, P. B. Littlewood, K. W. West, M. J. Matthews, and J. Wynn, cond-mat/0206125 (unpublished).
- ¹⁴H. Akiyama, L. N. Pfeiffer, A. Pinczuk, K. W. West, and M. Yoshita, Solid State Commun. **122**, 169 (2002).
- ¹⁵The observed positive oscillating charge is assumed to be smaller than the negative charge because the mobility of free holes, compared with the one of free electrons, is remarkably smaller.